Article

Synchronization of Nonlinear Complex Spatiotemporal Networks Based on PIDEs with Multiple Time Delays: A P-sD Method

Jiashu Dai [1,†] and Chengdong Yang [2,*,†]

1   School of Computer and Information, Anhui Polytechnic University, Wuhu 241000, China;
     daijiashudai@ahpu.edu.cn
2   School of Information Science and Technology, Linyi University, Linyi 276005, China
*   Correspondence: yangchengdong@lyu.edu.cn
†   These authors contributed equally to this work.

Abstract: This paper studies the synchronization control of nonlinear multiple time-delayed complex spatiotemporal networks (MTDCSNs) based on partial integro-differential equations. Firstly, dealing with an MTDCSN with time-invariant delays, P-sD control is employed and the synchronization criteria are obtained in terms of LMIs. Secondly, this control method is further used in an MTDCSN with time-varying delays. An example illustrates the effectiveness of the proposed methods.

Keywords: complex spatiotemporal networks; synchronization; LMIs; partial integro-differential equations

1. Introduction

As a typical collective behavior in nature, the synchronization of complex networks has attracted a great deal of attention during the last few decades [1–3]. It has been widely applied to engineering fields, such as secure communication [4,5], deception attacks [6–8], the design of pseudorandom number generators [9], and image encryption [10].

In fact, many phenomena rely not only on time but also on space [11–13]. As a result, many researchers have studied complex spatiotemporal networks (CSNs), owing to many phenomena relating not only to time but also to space. Kanakov et al. studied the cluster synchronization of the CSNs of oscillatory and excitable Luo–Rudy cells [14]. Kakmeni and Baptista proposed synchronization and information transmission in CSNs under a substrate Remoissenet–Peyrard potential [15]. Rybalova et al. investigated complete synchronization under the condition of spatio-temporal chaos with the Henon map and Lozi map [16]. Yang et al. studied the guaranteed cost boundary control of nonlinear CSNs with a community structure [17] and the boundary control of CSNs modeled by partial differential equations–ordinary differential Equations (PDE-ODEs) [18].

Owing to the extensive existence of time delays, it is important to research time-delayed networks [19–22]. Yao et al. studied the passive stability and synchronization of switching CSNs with time delays in terms of appropriate algebraic inequalities [23,24]. Zhou et al. proposed two methods—matrix invertibility and an adaptive law—for the topology identification and finite-time topology identification of time-delayed complex spatiotemporal networks (TDCSNs) [25,26]. Sheng et al. studied the exponential synchronization of TDCSNs with Dirichlet boundary conditions and hybrid time delays via impulsive control [27]. Lu et al. studied generalized sampled-data intermittent control for the exponential synchronization of TDCSNs [28]. Yang et al. proposed the synchronization of nonlinear complex spatio-temporal networks with multiple time-invariant delays and multiple time-varying delays [29]. Zhang et al. proposed fuzzy time sampled-data control and fuzzy time–space sampled-data control for the synchronization of T–S fuzzy TDCSNs with additive time-varying delays [30].

On the whole, most of the mentioned literature assumes that nodes are modeled by partial differential equations, PDEs, or PDE-ODEs. Few studies consider models based on partial integro-differential Equations (PIDEs). PIDEs have been applied to spread and traveling waves [31], pricing models [32], biology [33], pattern formation [34], secure communication [5], and medical science [35]. Many dynamical behaviors of PIDEs have been studied [36–38]. However, there are still some technical difficulties in the synchronization of multiple time-delayed TDCSNs based on PIDEs, such as communication among nodes and controller design, which is the motivation for this paper.

Notations: I means an identity matrix with proper order; $P < 0$ is a negative definite matrix, while $P > 0$ is positive definite; '*' is an ellipsis of transpose blocks in symmetric matrices.

2. Problem Formulation

This paper studies a class of nonlinear MTDCSNs based on PIDEs:

$$
\begin{aligned}
\frac{\partial y_i(\zeta,t)}{\partial t} &= \Theta_1 \frac{\partial^2 y_i(\zeta,t)}{\partial \zeta^2} + \Theta_2 \frac{\partial y_i(\zeta,t)}{\partial \zeta} + A y_i(\zeta, t - \tau_1(t)) + f(y_i(\zeta, t - \tau_2(t))) \\
&\quad + B \int_0^\zeta y_i(z, t - \tau_3(t)) dz + c \sum_{j=1}^N h_{ij} \Gamma y_j(\zeta, t - \tau_4(t)) + u_i(\zeta, t), \\
\frac{\partial y_i(0,t)}{\partial \zeta} &= 0, \frac{\partial y_i(L,t)}{\partial \zeta} = 0, \\
y_i(\zeta,t) &= y_i^0(\zeta,t), (\zeta,t) \in [0,L] \times [-\tau, 0],
\end{aligned}
\tag{1}
$$

where $(\zeta, t) \in [0, L] \times [0, \infty)$. Here, $y_i(\zeta, t), u_i(\zeta, t) \in \mathbb{R}^n$ are the respective state and control inputs, $i \in \{1, 2, \cdots, N\}$. $\Theta_1 \in \mathbb{R}^{n \times n}$ is the diffusion coefficient matrix. $\Theta_2 \in \mathbb{R}^{n \times n}$ is the convection coefficient matrix. $A \in \mathbb{R}^{n \times n}$ and $B \in \mathbb{R}^{n \times n}$ are the connection matrices. $0 < \Gamma \in \mathbb{R}^{n \times n}$ is the inner coupling matrix. The coupling strength c is a positive real number. The coupling connection $H = (h_{ij})_{N \times N}$ is defined as $h_{ij} > 0 (i \neq j)$ if the agent j connects to i and $h_{ii} = -\sum_{j \neq i} h_{ij}$. $f(\cdot)$ is a nonlinear function that varies over time and space. $0 < \tau_1(t), \tau_2(t), \tau_3(t), \tau_4(t) \le \tau, \dot{\tau}_1(t) \le \mu_1, \dot{\tau}_2(t) \le \mu_2, \dot{\tau}_3(t) \le \mu_3$, and $\dot{\tau}_4(t) \le \mu_4$.

The isolated node is supposed to be:

$$
\begin{aligned}
\frac{\partial s(\zeta,t)}{\partial t} &= \Theta_1 \frac{\partial^2 s(\zeta,t)}{\partial \zeta^2} + \Theta_2 \frac{\partial s(\zeta,t)}{\partial \zeta} + A s(\zeta, t - \tau_1(t)) + f(s(\zeta, t - \tau_2(t))) \\
&\quad + B \int_0^\zeta s(z, t - \tau_3(t)) dz, \\
\frac{\partial s(0,t)}{\partial \zeta} &= 0, \frac{\partial s(L,t)}{\partial \zeta} = 0, \\
s(\zeta,t) &= s^0(\zeta,t), (\zeta,t) \in [0,L] \times [-\tau, 0].
\end{aligned}
\tag{2}
$$

We denote the synchronization error as $\epsilon_i(\zeta, t) \stackrel{\Delta}{=} y_i(\zeta, t) - s(\zeta, t)$. The P-sD controller is designed as

$$
u_i(\zeta, t) = -K_{Pi} \epsilon_i(\zeta, t) - K_{Di} \frac{\partial \epsilon_i(\zeta, t)}{\partial \zeta},
\tag{3}
$$

where $K_{Pi}, K_{Di} \in \mathbb{R}^{n \times n}$, $i \in \{1, 2, \cdots, N\}$, need to be determined. The controller structure in this paper is shown in Figure 1, where the notation "$\partial/\partial \zeta$" represents a first-order spatial differentiator. With (3), the error system of the MTDCSN (1) can be obtained as:

$$\frac{\partial \epsilon_i(\zeta,t)}{\partial t} = \Theta_1 \frac{\partial^2 \epsilon_i(\zeta,t)}{\partial \zeta^2} + \Theta_2 \frac{\partial \epsilon_i(\zeta,t)}{\partial \zeta} - K_{Di} \frac{\partial \epsilon_i(\zeta,t)}{\partial \zeta} - K_{Pi}\epsilon_i(\zeta,t)$$
$$+ A\epsilon_i(\zeta,t-\tau_1(t)) + F(\epsilon_i(\zeta,t-\tau_2(t)))$$
$$+ B\int_0^\zeta \epsilon_i(s,t-\tau_3(t))ds + c\sum_{j=1}^N h_{ij}\Gamma\epsilon_j(\zeta,t-\tau_4(t)), \qquad (4)$$
$$\frac{\partial \epsilon_i(0,t)}{\partial \zeta} = 0, \frac{\partial \epsilon_i(L,t)}{\partial \zeta} = 0,$$
$$\epsilon_i(\zeta,t) = \epsilon_i^0(\zeta,t), (\zeta,t)\in[0,L]\times[-\tau,0],$$

where $F(\epsilon_i(\zeta,t-\tau_2(t))) \triangleq f(y_i(\zeta,t-\tau_2(t))) - f(s(\zeta,t-\tau_2(t))), \epsilon_i^0(\zeta) \triangleq y_i^0(\zeta) - s^0(\zeta).$
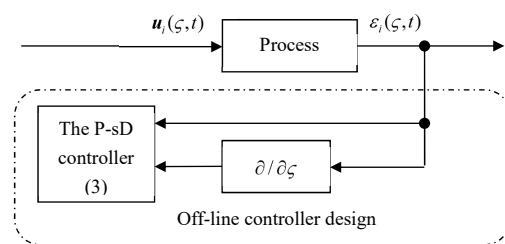
Figure 1. The structure of the P-sD controller (3).

Assumption 1. *For any a,b, assume there exists a scalar $\chi > 0$ satisfying:*

$$|f(a)-f(b)| \leqslant \chi|a-b|. \qquad (5)$$

Lemma 1. *([39]) For any square integral vector ϵ with $\epsilon(0)=0$ and $\epsilon(L)=0$,*

$$\int_0^L \epsilon^T(z)\epsilon(z)dz \leq L^2\pi^{-2}\int_0^L \dot\epsilon^T(z)\dot\epsilon(z)dz. \qquad (6)$$

This paper aims to use the controller (3) to achieve the synchronization of the MTD-CSN (1) with the isolated node (2).

3. Synchronization of the MTDCSN with Time-Invariant Delays

We firstly researched the MTDCSN (1) with time-invariant delays, whose error system yields:

$$\frac{\partial \epsilon_i(\zeta,t)}{\partial t} = \Theta_1 \frac{\partial^2 \epsilon_i(\zeta,t)}{\partial \zeta^2} + \Theta_2 \frac{\partial \epsilon_i(\zeta,t)}{\partial \zeta} - K_{Di} \frac{\partial \epsilon_i(\zeta,t)}{\partial \zeta} - K_{Pi}\epsilon_i(\zeta,t)$$
$$+ A\epsilon_i(\zeta,t-\tau_1) + F(\epsilon_i(\zeta,t-\tau_2))$$
$$+ B\int_0^\zeta \epsilon_i(s,t-\tau_3)ds + c\sum_{j=1}^N h_{ij}\Gamma\epsilon_j(\zeta,t-\tau_4), \qquad (7)$$
$$\frac{\partial \epsilon_i(0,t)}{\partial \zeta} = 0, \frac{\partial \epsilon_i(L,t)}{\partial \zeta} = 0,$$
$$\epsilon_i(\zeta,t) = \epsilon_i^0(\zeta,t), (\zeta,t)\in[0,L]\times[-\tau,0].$$

Theorem 1. *Given the MTDCSN (1) with time-invariant delays, the MTDCSN (1) synchronizes with the isolated node (2) under the control (3) if there are scalars $\alpha_i > 0$, M_{Pi}, $M_{Di} \in \mathbb{R}^{n \times n}$ and symmetric positive definite matrices R_i, $S_i \in \mathbb{R}^{n \times n}$ satisfying the following LMIs:*

$$\Psi_1 \triangleq \begin{bmatrix} \Psi_{11} & (I_N \otimes \Theta_2)\bar{R} - \bar{M}_D & (I_N \otimes A)\bar{R} & (cH \otimes \Gamma)\bar{R} \\ * & -[(I_N \otimes \Theta_1)\bar{R} + *] & 0 & 0 \\ * & * & -\bar{S} & 0 \\ * & * & * & -\bar{S} \end{bmatrix} < 0 \tag{8}$$

$$\Psi_2 \triangleq \begin{bmatrix} -\bar{S} & \bar{R} \\ * & -\chi^{-2}\bar{\alpha} \otimes I_n \end{bmatrix} < 0, \tag{9}$$

$$\Psi_3 \triangleq \begin{bmatrix} -\bar{S} & \bar{R} \\ * & -L^{-2}\pi^2\bar{\alpha} \otimes I_n \end{bmatrix} < 0, \tag{10}$$

where $\Psi_{11} \triangleq -[\bar{M}_P + *] + \bar{\alpha} \otimes I_n + \bar{\alpha} \otimes BB^T + 4\bar{S}$, $\bar{\alpha} = diag\{\alpha_1, \alpha_2, \cdots, \alpha_N\}$, $\bar{P} = diag\{P_1, P_2, \cdots, P_N\}$, $\bar{Q} \triangleq diag\{Q_1, Q_2, \cdots, Q_N\}$, $\bar{M}_P \triangleq diag\{M_{P1}, M_{P2}, \cdots, M_{PN}\}$, *and* $\bar{M}_D \triangleq diag\{M_{D1}, M_{D2}, \cdots, M_{DN}\}$. *In this case,* $K_{Pi} = M_{Pi}R_i^{-1}$ *and* $K_{Di} = M_{Di}R_i^{-1}$.

Proof. We choose the Lyapunov functional candidate as:

$$V(t) = V_1(t) + V_2(t), \tag{11}$$

where:

$$V_1(t) = \int_0^L \epsilon^T(\zeta, t)\bar{P}\epsilon(\zeta, t)d\zeta,$$

$$V_2(t) = \int_0^L \int_{t-\tau_1}^t \epsilon^T(\zeta, \rho)\bar{Q}\epsilon(\zeta, \rho)d\rho d\zeta$$

$$+ \int_0^L \int_{t-\tau_2}^t \epsilon^T(\zeta, \rho)\bar{Q}\epsilon(\zeta, \rho)d\rho d\zeta \tag{12}$$

$$+ \int_0^L \int_{t-\tau_3}^t \epsilon^T(\zeta, \rho)\bar{Q}\epsilon(\zeta, \rho)d\rho d\zeta$$

$$+ \int_0^L \int_{t-\tau_4}^t \epsilon^T(\zeta, \rho)\bar{Q}\epsilon(\zeta, \rho)d\rho d\zeta,$$

in which $\epsilon(\zeta, t) \triangleq [\epsilon_1^T(\zeta, t), \epsilon_2^T(\zeta, t), \cdots, \epsilon_N^T(\zeta, t)]^T$.

Taking the time derivative of $V_1(t)$:

$$
\begin{aligned}
\dot{V}_1(t) =& 2\int_0^L \epsilon^T(\zeta,t)\frac{\partial \epsilon(\zeta,t)}{\partial t}d\zeta \\
=& 2\int_0^L \epsilon^T(\zeta,t)\bar{P}(I_N \otimes \Theta_1)\frac{\partial^2 \epsilon(\zeta,t)}{\partial \zeta^2}d\zeta \\
& + 2\int_0^L \epsilon^T(\zeta,t)\bar{P}(I_N \otimes \Theta_2)\frac{\partial \epsilon(\zeta,t)}{\partial \zeta}d\zeta \\
& - 2\int_0^L \epsilon^T(\zeta,t)\bar{P}\bar{K}_D\frac{\partial \epsilon(\zeta,t)}{\partial \zeta}d\zeta \\
& - 2\int_0^L \epsilon^T(\zeta,t)\bar{P}\bar{K}_P\epsilon(\zeta,t)d\zeta \\
& + 2\int_0^L \epsilon^T(\zeta,t)\bar{P}(I_N \otimes A)\epsilon(\zeta,t-\tau_1)d\zeta \\
& + 2\int_0^L \epsilon^T(\zeta,t)\bar{P}(cH \otimes \Gamma)\epsilon(\zeta,t-\tau_4)d\zeta \\
& + 2\int_0^L \epsilon^T(\zeta,t)\bar{P}F(\epsilon(\zeta,t-\tau_2))d\zeta \\
& + 2\int_0^L \epsilon^T(\zeta,t)\bar{P}(I_N \otimes B)\int_0^\zeta \epsilon(z,t-\tau_3)dzd\zeta.
\end{aligned}
\tag{13}
$$

By integrating by parts:

$$
\begin{aligned}
& 2\int_0^L \epsilon^T(\zeta,t)\bar{P}(I_N \otimes \Theta_1)\frac{\partial^2 \epsilon(\zeta,t)}{\partial \zeta^2}d\zeta \\
=& -\int_0^L \frac{\partial \epsilon(\zeta,t)}{\partial \zeta}[\bar{P}(I_N \otimes \Theta_1) + *]\frac{\partial \epsilon(\zeta,t)}{\partial \zeta}d\zeta.
\end{aligned}
\tag{14}
$$

Using Assumption 1, for any $\alpha_i > 0$:

$$
\begin{aligned}
& 2\int_0^L \epsilon^T(\zeta,t)\bar{P}F(\epsilon(\zeta,t-\tau_2))d\zeta \\
\leqslant& \sum_{i=1}^N \alpha_i \int_0^L \epsilon_i^T(\zeta,t)P_i P_i \epsilon_i(\zeta,t)d\zeta \\
& + \sum_{i=1}^N \alpha_i^{-1}\int_0^L F^T(\epsilon_i(\zeta,t-\tau_2)F(\epsilon_i(\zeta,t-\tau_2))d\zeta \\
\leqslant& \sum_{i=1}^N \alpha_i \int_0^L \epsilon_i^T(\zeta,t)\bar{P}_i \bar{P}_i \epsilon_i(\zeta,t)d\zeta \\
& + \sum_{i=1}^N \alpha_i^{-1}\chi^2 \int_0^L \epsilon_i^T(\zeta,t-\tau_2)\epsilon_i(\zeta,t-\tau_2)d\zeta.
\end{aligned}
\tag{15}
$$

Using Lemma 1, for any $\alpha_i > 0$:

$$2 \int_0^L \epsilon^T(\zeta, t) \bar{P}(I_N \otimes B) \int_0^\zeta \epsilon(z, t - \tau_3) dz d\zeta$$

$$\leqslant \sum_{i=1}^N \alpha_i \int_0^L \epsilon_i^T(\zeta, t) \bar{P}_i BB^T \bar{P}_i \epsilon_i(\zeta, t) d\zeta$$

$$+ \sum_{i=1}^N \alpha_i^{-1} \int_0^L \int_0^\zeta \epsilon_i^T(z, t - \tau_3) dz \int_0^\zeta \epsilon_i(z, t - \tau_3) dz d\zeta \qquad (16)$$

$$\leqslant \sum_{i=1}^N \alpha_i \int_0^L \epsilon_i^T(\zeta, t) P_i BB^T P_i \epsilon_i(\zeta, t) d\zeta$$

$$+ L^2 \pi^{-2} \sum_{i=1}^N \alpha_i^{-1} \int_0^L \epsilon_i^T(\zeta, t - \tau_3) \epsilon_i(\zeta, t - \tau_3) d\zeta.$$

Taking the time derivative of $V_2(t)$:

$$\dot{V}_2(t) = 4 \int_0^L \epsilon^T(\zeta, t) \bar{Q} \epsilon(\zeta, t) d\zeta$$

$$- \int_0^L \epsilon^T(\zeta, t - \tau_1) \bar{Q} \epsilon(\zeta, t - \tau_1) d\zeta$$

$$- \int_0^L \epsilon^T(\zeta, t - \tau_2) \bar{Q} \epsilon(\zeta, t - \tau_2) d\zeta \qquad (17)$$

$$- \int_0^L \epsilon^T(\zeta, t - \tau_3) \bar{Q} \epsilon(\zeta, t - \tau_3) d\zeta$$

$$- \int_0^L \epsilon^T(\zeta, t - \tau_4) \bar{Q} \epsilon(\zeta, t - \tau_4) d\zeta.$$

Substituting (13)–(17) into the time derivative of $V(t)$ yields:

$$\dot{V}(t) \leqslant \int_0^L \tilde{\epsilon}^T(\zeta, t) \bar{\Psi} \tilde{\epsilon}(\zeta, t) d\zeta + \int_0^L \epsilon^T(\zeta, t - \tau_2) \bar{\Psi}_1 \epsilon(\zeta, t - \tau_2) d\zeta$$

$$+ \int_0^L \epsilon^T(\zeta, t - \tau_3) \bar{\Psi}_2 \epsilon(\zeta, t - \tau_3) d\zeta, \qquad (18)$$

where $\tilde{\epsilon}(\zeta, t) \triangleq [\epsilon^T(\zeta, t), \frac{\partial \epsilon^T(\zeta, t)}{\partial \zeta}, \epsilon^T(\zeta, t - \tau_1), \epsilon^T(\zeta, t - \tau_4)]^T$, and:

$$\bar{\Psi}_1 \triangleq \begin{bmatrix} \bar{\Psi}_{11} & \bar{P}(I_N \otimes \Theta_2) - K_D \bar{P} & \bar{P}(I_N \otimes A) & c\bar{P}(H \otimes \Gamma) \\ * & -\bar{P}[I_N \otimes \Theta_1 + *] & 0 & 0 \\ * & * & -\bar{Q} & 0 \\ * & * & * & -\bar{Q} \end{bmatrix}, \qquad (19)$$

$$\bar{\Psi}_2 \triangleq -\bar{Q} + \chi^2 (\bar{\alpha}^{-1} \otimes I_n), \qquad (20)$$

$$\bar{\Psi}_3 \triangleq -\bar{Q} + L^2 \pi^{-2} (\bar{\alpha}^{-1} \otimes I_n), \qquad (21)$$

in which

$$\Psi_{11} \triangleq -[\bar{P}\bar{K}_P + *] + \bar{P}(\bar{\alpha} \otimes I_n)\bar{P} + \bar{P}(\bar{\alpha} \otimes BB^T)\bar{P} + 4\bar{Q}.$$

Pre- and post-multiplying (19) by $diag\{P^{-1}, \bar{P}^{-1}, \bar{P}^{-1}, \bar{P}^{-1}\}$, (20) by $\bar{P}^{-1}$, and (21) by $\bar{P}^{-1}$, respectively, one has:

$$\hat{\Psi}_1 \triangleq \begin{bmatrix} \hat{\Psi}_{11} & \hat{\Psi}_{12} & (I_N \otimes A)\bar{P}^{-1} & (cH \otimes \Gamma)\bar{P}^{-1} \\ * & -[(I_N \otimes \Theta_1)\bar{P}^{-1} + *] & 0 & 0 \\ * & * & -\bar{P}^{-1}\bar{Q}\bar{P}^{-1} & 0 \\ * & * & * & -\bar{P}^{-1}\bar{Q}\bar{P}^{-1} \end{bmatrix}, \quad (22)$$

$$\hat{\Psi}_2 \triangleq -\bar{P}^{-1}\bar{Q}P^{-1} + \chi^2\bar{P}^{-1}(\bar{\alpha}^{-1} \otimes I_n)\bar{P}^{-1}, \quad (23)$$

$$\hat{\Psi}_3 \triangleq -\bar{P}^{-1}\bar{Q}\bar{P}^{-1} + L^2\pi^{-2}\bar{P}^{-1}(\bar{\alpha}^{-1} \otimes I_n)\bar{P}^{-1}, \quad (24)$$

in which:

$$\hat{\Psi}_{11} \triangleq -[\bar{K}_P\bar{P}^{-1} + *] + \bar{\alpha} \otimes I_n + \bar{\alpha} \otimes BB^T + 4P^{-1}\bar{Q}\bar{P}^{-1},$$

$$\hat{\Psi}_{12} \triangleq (I_N \otimes \Theta_2)\bar{P}^{-1} - \bar{K}_D\bar{P}^{-1}.$$

Setting $P_i^{-1} = R_i, K_{Di}P_i^{-1} = M_{Di}, K_{Pi}P_i^{-1} = M_{Pi}, P_i^{-1}Q_iP_i^{-1} = S_i$, one has (22) < 0 if and only if (8) < 0, (23) < 0 if and only if (9) < 0, and (24) < 0 if and only if (10) < 0. Since (8)–(10) hold, $\dot{V}(t) \leq -\kappa||\tilde{\epsilon}(\cdot, t)|| \leq -\kappa||\epsilon(\cdot, t)||$ for all non-zero $\epsilon(\cdot, t)$, where κ is the minimal eigenvalue of $-\Psi$, which ensures the synchronization of the MTDCSN (1) with the isolated node (2). $\square$

4. Synchronization of the MTDCSN with Time-Varying Delays

Theorem 2. *Given the MTDCSN (1) with time-varying delays, the MTDCSN (1) synchronizes with the isolated node (2) under the controller (3), if there are scalars $\alpha_i > 0$, matrices M_{Pi}, $M_{Di} \in \mathbb{R}^{n \times n}$, and symmetric positive definite matrices R_i, $S_i \in \mathbb{R}^{n \times n}$ satisfying the following LMIs:*

$$\Xi_1 \triangleq \begin{bmatrix} \Xi_{11} & \Xi_{12} & (I_N \otimes A)\bar{R} & (cH \otimes \Gamma)\bar{R} \\ * & -[(I_N \otimes \Theta_1)\bar{R} + *] & 0 & 0 \\ * & * & -(1 - \mu_1)\bar{S} & 0 \\ * & * & * & -(1 - \mu_4)\bar{S} \end{bmatrix} < 0, \quad (25)$$

$$\Xi_2 \triangleq \begin{bmatrix} -(1 - \mu_2)\bar{S} & \bar{R} \\ * & -\chi^{-2}\bar{\alpha} \otimes I_n \end{bmatrix} < 0, \quad (26)$$

$$\Xi_3 \triangleq \begin{bmatrix} -(1 - \mu_3)\bar{S} & \bar{R} \\ * & -L^{-2}\pi^2\bar{\alpha} \otimes I_n \end{bmatrix} < 0, \quad (27)$$

where $\Xi_{11} \triangleq -[\bar{M}_P + *] + \bar{\alpha} \otimes I_n + \bar{\alpha} \otimes BB^T + 4\bar{S}$, $\Xi_{12} \triangleq (I_N \otimes \Theta_2)\bar{R} - \bar{M}_D$, $\bar{\alpha} = diag\{\alpha_1, \alpha_2, \cdots, \alpha_N\}$, $\bar{P} = diag\{P_1, P_2, \cdots, P_N\}$, $\bar{Q} \triangleq diag\{Q_1, Q_2, \cdots, Q_N\}$, $\bar{M}_P \triangleq diag\{M_{P1}, M_{P2}, \cdots, M_{PN}\}$, and $\bar{M}_D \triangleq diag\{M_{D1}, M_{D2}, \cdots, M_{DN}\}$. In this case, $K_{Pi} = M_{Pi}R_i^{-1}, K_{Di} = M_{Di}R_i^{-1}$.

Proof. We choose the Lyapunov functional candidate as:

$$V(t) = V_1(t) + V_3(t), \quad (28)$$

where:

$$\begin{aligned} V_3(t) = &\int_0^L \int_{t-\tau_1(t)}^t \epsilon^T(\zeta, \rho)\bar{Q}\epsilon(\zeta, \rho)d\rho d\zeta \\ &+ \int_0^L \int_{t-\tau_2(t)}^t \epsilon^T(\zeta, \rho)\bar{Q}\epsilon(\zeta, \rho)d\rho d\zeta \\ &+ \int_0^L \int_{t-\tau_3(t)}^t \epsilon^T(\zeta, \rho)\bar{Q}\epsilon(\zeta, \rho)d\rho d\zeta \\ &+ \int_0^L \int_{t-\tau_4(t)}^t \epsilon^T(\zeta, \rho)\bar{Q}\epsilon(\zeta, \rho)d\rho d\zeta. \end{aligned} \quad (29)$$

Taking the time derivative of $V_3(t)$:

$$
\begin{aligned}
\dot{V}_3(t) &= 4\int_0^L \epsilon^T(\zeta,t)\bar{Q}\epsilon(\zeta,t)d\zeta \\
&\quad -(1-\dot{\tau}_1(t))\int_0^L \epsilon^T(\zeta,t-\tau_1(t))\bar{Q}\epsilon(\zeta,t-\tau_1(t))d\zeta \\
&\quad -(1-\dot{\tau}_2(t))\int_0^L \epsilon^T(\zeta,t-\tau_2(t))\bar{Q}\epsilon(\zeta,t-\tau_2(t))d\zeta \\
&\quad -(1-\dot{\tau}_3(t))\int_0^L \epsilon^T(\zeta,t-\tau_3(t))\bar{Q}\epsilon(\zeta,t-\tau_3(t))d\zeta \\
&\quad -(1-\dot{\tau}_4(t))\int_0^L \epsilon^T(\zeta,t-\tau_3(t))\bar{Q}\epsilon(\zeta,t-\tau_4(t))d\zeta \\
&\leqslant 4\int_0^L \epsilon^T(\zeta,t)\bar{Q}\epsilon(\zeta,t)d\zeta \\
&\quad -(1-\mu_1)\int_0^L \epsilon^T(\zeta,t-\tau_1(t))\bar{Q}\epsilon(\zeta,t-\tau_1(t))d\zeta \\
&\quad -(1-\mu_2)\int_0^L \epsilon^T(\zeta,t-\tau_2(t))\bar{Q}\epsilon(\zeta,t-\tau_2(t))d\zeta \\
&\quad -(1-\mu_3)\int_0^L \epsilon^T(\zeta,t-\tau_3(t))\bar{Q}\epsilon(\zeta,t-\tau_3(t))d\zeta \\
&\quad -(1-\mu_4)\int_0^L \epsilon^T(\zeta,t-\tau_3(t))\bar{Q}\epsilon(\zeta,t-\tau_4(t))d\zeta.
\end{aligned}
\tag{30}
$$

The latter part of this proof is similar to that of Theorem 1 and so is omitted. □

Remark 1. *It is obvious that Theorem 2 is suitable only for situations where there is no quickly increasing time delay, since LMIs (25)–(27) imply $\mu_1 < 1, \mu_2 < 1, \mu_3 < 1, \mu_4 < 1$, i.e., $\dot{\tau}_1(t) < 1, \dot{\tau}_2(t) < 1, \dot{\tau}_3(t) < 1, \dot{\tau}_4(t) < 1$.*

Remark 2. *Different from the synchronization for TDCSNs [23–30] modeled by PDEs, the MTD-CSNs studied in this paper are modeled by PIDEs.*

Remark 3. *Different from the SPID control for the exponential stabilization of complex PIDE networks with a single time delay [40], this paper deals with the synchronization of the MTDCSN based on PIDEs with multiple time delays existing in the state, communication, nonlinear term, and integral term.*

5. Numerical Simulation

Example 1. *Consider the MTDCSN (1) with random initial conditions and the following parameters:*

$$
\Theta_1 = \begin{bmatrix} 1 & 0 \\ 0 & 4 \end{bmatrix}, \Theta_2 = \begin{bmatrix} 1 & 0 \\ 0 & 1.2 \end{bmatrix}, A = \begin{bmatrix} 2.2 & -0.2 \\ 0.5 & 1 \end{bmatrix},
$$

$$
B = \begin{bmatrix} 2 & 0 \\ 0 & 2 \end{bmatrix}, L = 1, c = 0.2,
$$

$$
\tau_1 = 1, \tau_2 = 2, \tau_3 = 1, \tau_4 = 2,
\tag{31}
$$

$$
H = \begin{bmatrix} -3 & 1 & 1 & 1 \\ 2 & -6 & 2 & 2 \\ 1 & 1 & -4 & 2 \\ 1 & 2 & 2 & -5 \end{bmatrix}.
$$

It is obvious that $\tau = \max\{\tau_1, \tau_2, \tau_3, \tau_4\} = 2$ and $\chi = 1$. From Figure 2, it can be seen that the MTDCSN (1) cannot achieve synchronization without control. According to Theorem 1, solving LMIs (8)–(10) with Matlab, we can obtain: $\alpha_1 = \alpha_2 = \alpha_3 = \alpha_4 = 11.8915$, and

$$
\begin{aligned}
R1 &= \begin{bmatrix} 1.0943 & -0.0033 \\ -0.0033 & 0.8875 \end{bmatrix}, R2 = \begin{bmatrix} 1.0894 & -0.0033 \\ -0.0033 & 0.8864 \end{bmatrix}, \\
R3 &= \begin{bmatrix} 1.0925 & -0.0033 \\ -0.0033 & 0.8871 \end{bmatrix}, R4 = \begin{bmatrix} 1.0909 & -0.0033 \\ -0.0033 & 0.8867 \end{bmatrix}, \\
S1 &= \begin{bmatrix} 1.0943 & -0.0033 \\ -0.0033 & 0.8875 \end{bmatrix}, S2 = \begin{bmatrix} 1.0894 & -0.0033 \\ -0.0033 & 0.8864 \end{bmatrix}, \\
S3 &= \begin{bmatrix} 1.0925 & -0.0033 \\ -0.0033 & 0.8871 \end{bmatrix}, S4 = \begin{bmatrix} 1.0909 & -0.0033 \\ -0.0033 & 0.8867 \end{bmatrix}.
\end{aligned}
\tag{32}
$$

Therefore, the control gains K_{Pi} and K_{Di} are obtained as:

$$
\begin{aligned}
K_{P1} &= \begin{bmatrix} 16.7885 & 0.0621 \\ 0.0621 & 20.7015 \end{bmatrix}, K_{P2} = \begin{bmatrix} 16.8639 & 0.0622 \\ 0.0622 & 20.7267 \end{bmatrix}, \\
K_{P3} &= \begin{bmatrix} 16.8164 & 0.0621 \\ 0.0621 & 20.7108 \end{bmatrix}, K_{P4} = \begin{bmatrix} 16.8416 & 0.0622 \\ 0.0622 & 20.7192 \end{bmatrix}, \\
K_{D1} &= \begin{bmatrix} 1.0000 & -0.0004 \\ 0.0003 & 1.2000 \end{bmatrix}, K_{D2} = \begin{bmatrix} 1.0000 & -0.0004 \\ 0.0003 & 1.2000 \end{bmatrix}, \\
K_{D3} &= \begin{bmatrix} 1.0000 & -0.0004 \\ 0.0003 & 1.2000 \end{bmatrix}, K_{D4} = \begin{bmatrix} 1.0000 & -0.0004 \\ 0.0003 & 1.2000 \end{bmatrix}.
\end{aligned}
\tag{33}
$$

It is shown in Figure 3 that the MTDCSN (1) achieves synchronization with the isolated node (2) under control with the gains (33). The controller is shown in Figure 4.
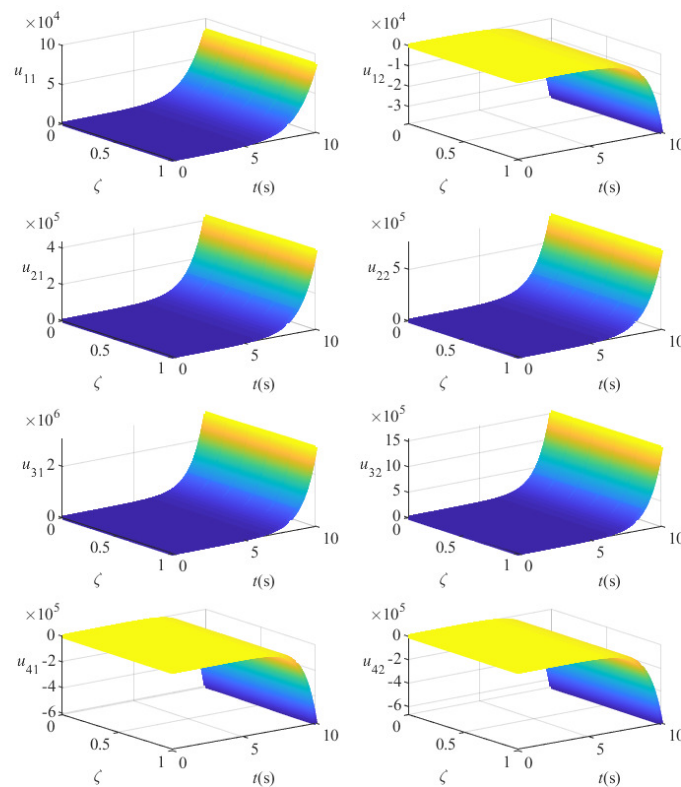
Figure 2. $\epsilon_i(\zeta, t)$ of the multiple time-delayed complex spatiotemporal network (MTDCSN) without control in Example 1.
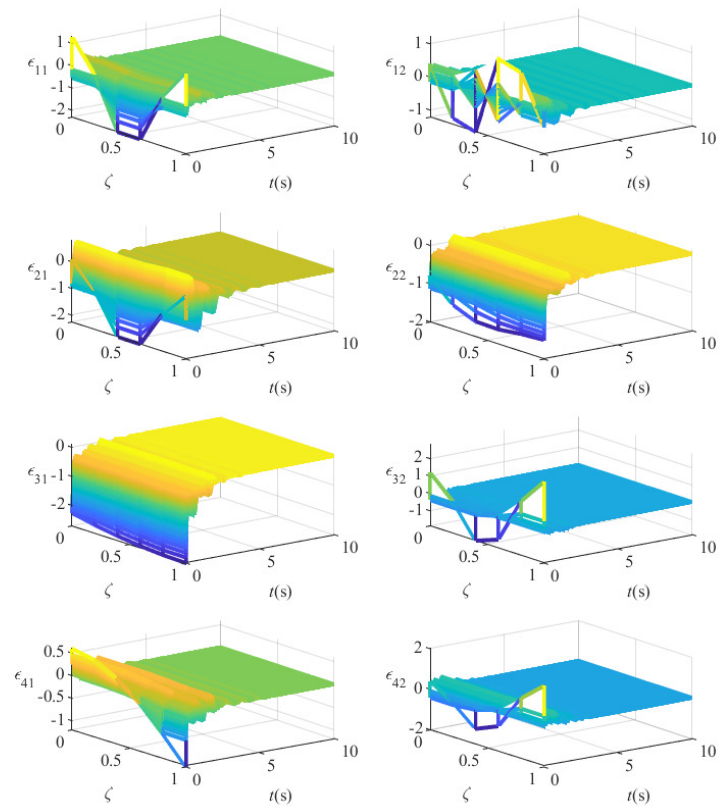
Figure 3. $\epsilon_i(\zeta, t)$ of the MTDCSN with control in Example 1.
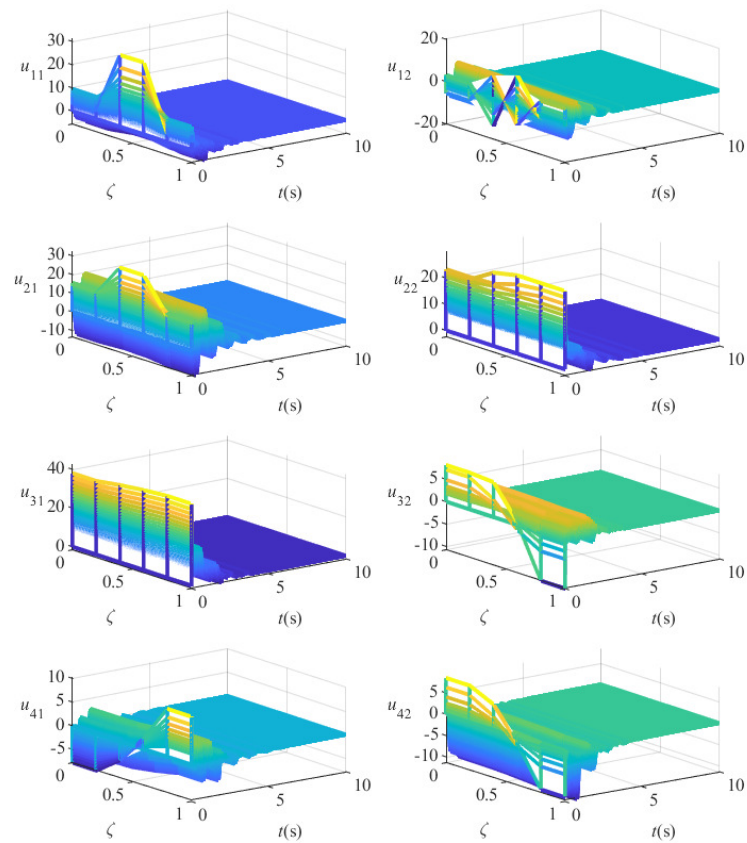
Figure 4. The controller $u_i(\zeta, t)$ in Example 1.

Example 2. *We consider the MTDCSN (1) with random initial conditions and the same parameters as those in Theorem 1, except:*

$$\tau_1(t) = 2 + sin(0.25\pi t), \tau_2(t) = 1 + 0.3cos(\pi t + \pi/4),$$
$$\tau_3(t) = 2 - \exp(-t/2), \tau_4(t) = 2 + 0.8\arctan(t). \tag{34}$$

We take $\max\{\tau_1(t), \tau_2(t), \tau_3(t), \tau_4(t)\} \leq \tau = 3$ *and* $\chi = 1$. *From (34), it is obvious that* $\mu_1 = 0.25\pi$, $\mu_2 = 0.3\pi$, $\mu_3 = 0.5$, $\mu_4 = 0.8$.

From Figure 5, it can be seen that the MTDCSN (1) cannot achieve synchronization without control. According to Theorem 2, solving LMIs (25)–(27) with Matlab, we can obtain: $\alpha_1 = \alpha_2 = \alpha_3 = \alpha_4 = 6.8606$, *and*

$$
\begin{aligned}
R1 &= \begin{bmatrix} 0.9737 & -0.0029 \\ -0.0029 & 0.7897 \end{bmatrix}, R2 = \begin{bmatrix} 0.9694 & -0.0029 \\ -0.0029 & 0.7887 \end{bmatrix}, \\
R3 &= \begin{bmatrix} 0.9721 & -0.0029 \\ -0.0029 & 0.7893 \end{bmatrix}, R4 = \begin{bmatrix} 0.9707 & -0.0029 \\ -0.0029 & 0.7890 \end{bmatrix}, \\
S1 &= \begin{bmatrix} 0.9737 & -0.0029 \\ -0.0029 & 0.7897 \end{bmatrix}, S2 = \begin{bmatrix} 0.9694 & -0.0029 \\ -0.0029 & 0.7887 \end{bmatrix}, \\
S3 &= \begin{bmatrix} 0.9721 & -0.0029 \\ -0.0029 & 0.7893 \end{bmatrix}, S4 = \begin{bmatrix} 0.9707 & -0.0029 \\ -0.0029 & 0.7890 \end{bmatrix}.
\end{aligned} \tag{35}
$$

Therefore, the control gains K_{Pi} *and* K_{Di} *are obtained as:*

$$
\begin{aligned}
K_{P1} &= \begin{bmatrix} 40.3444 & 0.1801 \\ 0.1511 & 47.6124 \end{bmatrix}, K_{P2} = \begin{bmatrix} 40.3914 & 0.1813 \\ 0.1523 & 47.6637 \end{bmatrix}, \\
K_{P3} &= \begin{bmatrix} 40.3605 & 0.1806 \\ 0.1516 & 47.6307 \end{bmatrix}, K_{P4} = \begin{bmatrix} 40.3762 & 0.1810 \\ 0.1520 & 47.6478 \end{bmatrix}, \\
K_{D1} &= \begin{bmatrix} 1.0000 & -0.0002 \\ 0.0000 & 1.2000 \end{bmatrix}, K_{D2} = \begin{bmatrix} 1.0000 & -0.0002 \\ 0.0000 & 1.2000 \end{bmatrix}, \\
K_{D3} &= \begin{bmatrix} 1.0000 & -0.0002 \\ 0.0000 & 1.2000 \end{bmatrix}, K_{D4} = \begin{bmatrix} 1.0000 & -0.0002 \\ 0.0000 & 1.2000 \end{bmatrix},
\end{aligned} \tag{36}
$$

It is shown in Figure 6 that the MTDCSN (1) achieves synchronization with the isolated node (2) under control with the gains (36). The controller is shown in Figure 7.
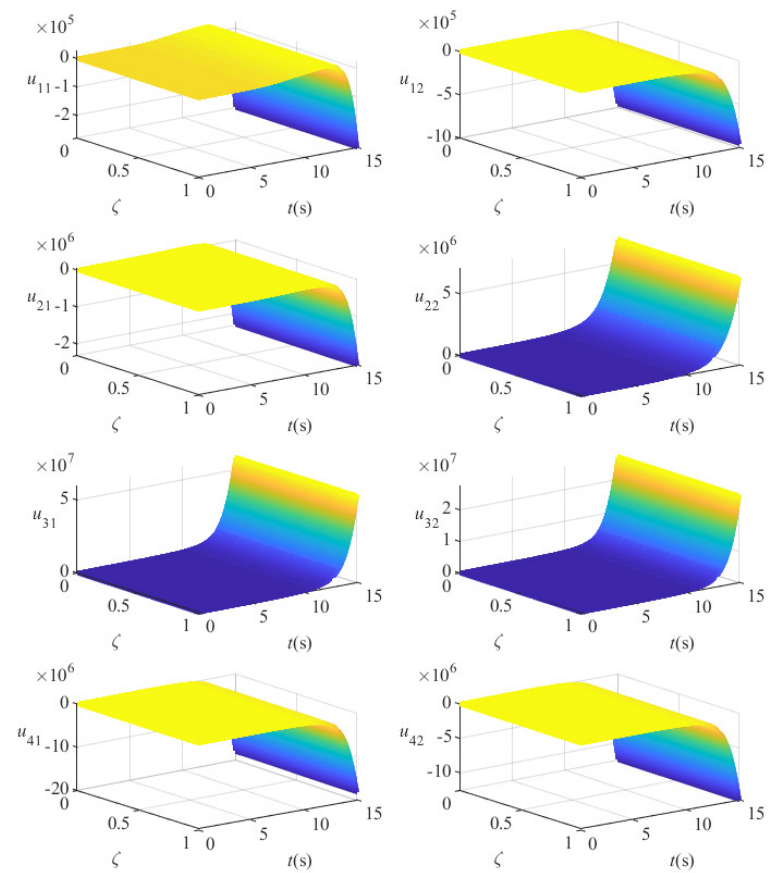
Figure 5. $\epsilon_i(\zeta, t)$ of the MTDCSN without control in Example 2.
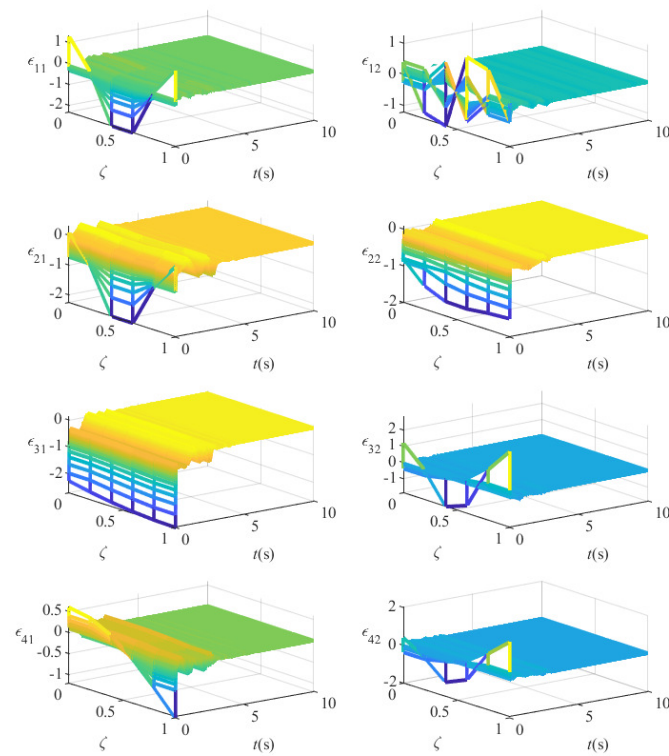
Figure 6. $\epsilon_i(\zeta, t)$ of the MTDCSN with control in Example 2.
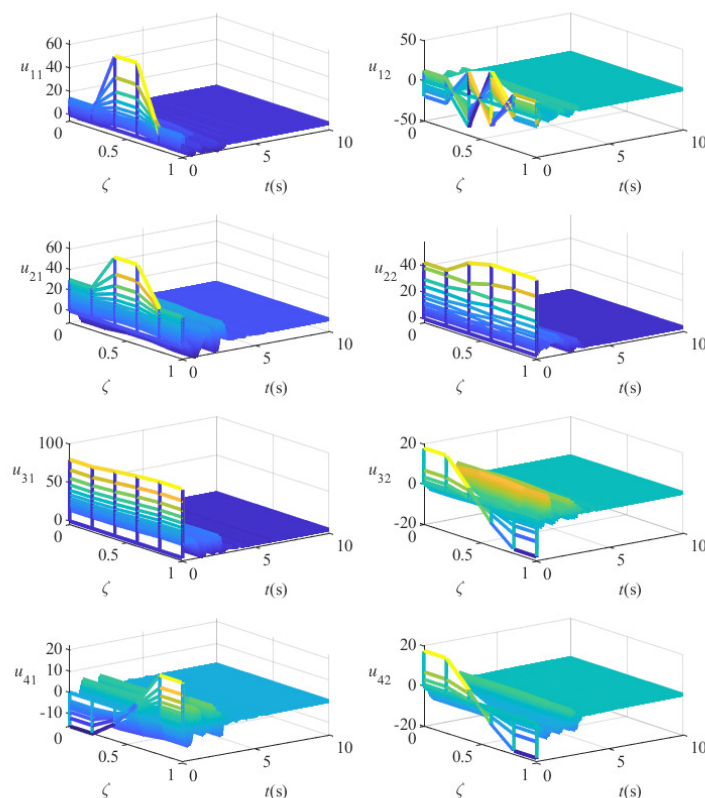
Figure 7. The controller $u_i(\zeta, t)$ in Example 2.

6. Conclusions

This paper aimed to study the synchronization of a class of nonlinear MTDCSNs. The model was established using coupled semi-linear parabolic PIDEs. P-sD control was employed for the MTDCSN with time-invariant delays and was further used for the MTDCSN with time-varying delays. The synchronization criteria were obtained in terms of LMIs for time-invariant delays and time-varying delays, respectively. An example was used to illustrate the effectiveness of the proposed methods. Compared with other methods, this method not only considers multiple time-invariant and time-varying delays but also deals with PIDE-based complex spatiotemporal networks. In future work, the pinning synchronization of MTDCSNs will be studied.

References

1. Hu, C.; He, H.; Jiang, H. Fixed/preassigned-time synchronization of complex networks via improving fixed-time stability. *IEEE Trans. Cybern.* **2020**, *51*, 2882–2892. [CrossRef]
2. Liu, X.; Ho, D.W.; Song, Q.; Xu, W. Finite/fixed-time pinning synchronization of complex networks with stochastic disturbances. *IEEE Trans. Cybern.* **2018**, *49*, 2398–2403. [CrossRef]
3. Gan, L.; Li, S.; Duan, N.; Kong, X. Adaptive output synchronization of general complex dynamical network with time-varying delays. *Mathematics* **2020**, *8*, 311. [CrossRef]
4. Alimi, A.M.; Aouiti, C.; Assali, E.A. Finite-time and fixed-time synchronization of a class of inertial neural networks with multi-proportional delays and its application to secure communication. *Neurocomputing* **2019**, *332*, 29–43. [CrossRef]

5. Shanmugam, L.; Mani, P.; Rajan, R.; Joo, Y.H. Adaptive synchronization of reaction–diffusion neural networks and its application to secure communication. *IEEE Trans. Cybern.* **2018**, *50*, 911–922. [CrossRef] [PubMed]

6. Dong, S.; Zhu, H.; Zhong, S.; Shi, K.; Lu, J. Impulsive-based almost surely synchronization for neural network systems subject to deception attacks. *IEEE Trans. Neural Netw. Learn. Syst.* **2021**. [CrossRef] [PubMed]

7. Zhang, H.; Li, L.; Li, X. Exponential synchronization of coupled neural networks under stochastic deception attacks. *Neural Netw.* **2022**, *145*, 189–198. [CrossRef]

8. Xing, M.; Lu, J.; Qiu, J.; Shen, H. Synchronization of complex dynamical networks subject to DoS attacks: An improved coding-decoding protocol. *IEEE Trans. Cybern.* **2021**. [CrossRef]

9. Wen, S.; Zeng, Z.; Huang, T.; Zhang, Y. Exponential adaptive lag synchronization of memristive neural networks via fuzzy method and applications in pseudorandom number generators. *IEEE Trans. Fuzzy Syst.* **2013**, *22*, 1704–1713. [CrossRef]

10. Mani, P.; Rajan, R.; Shanmugam, L.; Joo, Y.H. Adaptive control for fractional order induced chaotic fuzzy cellular neural networks and its application to image encryption. *Inf. Sci.* **2019**, *491*, 74–89. [CrossRef]

11. Feng, Y.; Wang, Y.; Wang, J.W.; Li, H.X. Backstepping-based distributed abnormality localization for linear parabolic distributed parameter systems. *Automatica* **2022**, *135*, 109930. [CrossRef]

12. Wu, H.N.; Zhang, X.M.; Wang, J.W.; Zhu, H.Y. Observer-based output feedback fuzzy control for nonlinear parabolic PDE-ODE coupled systems. *Fuzzy Sets Syst.* **2021**, *402*, 105–123. [CrossRef]

13. Wang, J.W. A unified Lyapunov-based design for a dynamic compensator of linear parabolic MIMO PDEs. *Int. J. Control* **2021**, *94*, 1804–1811. [CrossRef]

14. Kanakov, O.; Osipov, G.; Chan, C.K.; Kurths, J. Cluster synchronization and spatio-temporal dynamics in networks of oscillatory and excitable Luo-Rudy cells. *Chaos Interdiscip. J. Nonlinear Sci.* **2007**, *17*, 015111. [CrossRef] [PubMed]

15. Kakmeni, F.M.; Baptista, M. Synchronization and information transmission in spatio-temporal networks of deformable units. *Pramana* **2008**, *70*, 1063–1076. [CrossRef]

16. Rybalova, E.; Semenova, N.; Strelkova, G.; Anishchenko, V. Transition from complete synchronization to spatio-temporal chaos in coupled chaotic systems with nonhyperbolic and hyperbolic attractors. *Eur. Phys. J. Spec. Top.* **2017**, *226*, 1857–1866. [CrossRef]

17. Yang, C.; Cao, J.; Huang, T.; Zhang, J.; Qiu, J. Guaranteed cost boundary control for cluster synchronization of complex spatio-temporal dynamical networks with community structure. *Sci. China Inf. Sci.* **2018**, *61*, 052203. [CrossRef]

18. Yang, C.; Li, Z.; Chen, X.; Zhang, A.; Qiu, J. Boundary control for exponential synchronization of reaction-diffusion neural networks based on coupled PDE-ODEs. *IFAC-PapersOnLine* **2020**, *53*, 3415–3420. [CrossRef]

19. Tan, X.; Cao, J.; Rutkowski, L. Distributed dynamic self-triggered control for uncertain complex networks with Markov switching topologies and random time-varying delay. *IEEE Trans. Netw. Sci. Eng.* **2019**, *7*, 1111–1120. [CrossRef]

20. Wang, Y.; Tian, Y.; Li, X. Global exponential synchronization of interval neural networks with mixed delays via delayed impulsive control. *Neurocomputing* **2021**, *420*, 290–298. [CrossRef]

21. Yang, S.; Guo, Z.; Wang, J. Global synchronization of multiple recurrent neural networks with time delays via impulsive interactions. *IEEE Trans. Neural Netw. Learn. Syst.* **2016**, *28*, 1657–1667. [CrossRef] [PubMed]

22. Popa, C.A.; Kaslik, E. Finite–time Mittag–Leffler synchronization of neutral–type fractional-order neural networks with leakage delay and time-varying delays. *Mathematics* **2020**, *8*, 1146. [CrossRef]

23. Yao, J.; Wang, H.O.; Guan, Z.H.; Xu, W. Stability and passivity of complex spatio-temporal switching networks with coupling delays. *IFAC Proc.* **2008**, *41*, 6638–6641. [CrossRef]

24. Yao, J.; Wang, H.O.; Guan, Z.H.; Xu, W. Passive stability and synchronization of complex spatio-temporal switching networks with time delays. *Automatica* **2009**, *45*, 1721–1728. [CrossRef]

25. Zhou, D.D.; Guan, Z.H.; Liao, R.Q.; Chi, M.; Xiao, J.W.; Jiang, X.W. Topology identification of a class of complex spatio-temporal networks with time delay. *IET Control Theory Appl.* **2017**, *11*, 611–618. [CrossRef]

26. Zhou, D.D.; Hu, B.; Guan, Z.H.; Liao, R.Q.; Xiao, J.W. Finite-time topology identification of complex spatio-temporal networks with time delay. *Nonlinear Dyn.* **2018**, *91*, 785–795. [CrossRef]

27. Sheng, Y.; Zeng, Z. Impulsive synchronization of stochastic reaction–diffusion neural networks with mixed time delays. *Neural Netw.* **2018**, *103*, 83–93. [CrossRef]

28. Lu, B.; Jiang, H.; Hu, C.; Abdurahman, A. Synchronization of hybrid coupled reaction–diffusion neural networks with time delays via generalized intermittent control with spacial sampled-data. *Neural Netw.* **2018**, *105*, 75–87. [CrossRef]

29. Yang, C.; Huang, T.; Yi, K.; Zhang, A.; Chen, X.; Li, Z.; Qiu, J.; Alsaadi, F.E. Synchronization for nonlinear complex spatio-temporal networks with multiple time-invariant delays and multiple time-varying delays. *Neural Process. Lett.* **2019**, *50*, 1051–1064. [CrossRef]

30. Zhang, R.; Zeng, D.; Park, J.H.; Lam, H.K.; Xie, X. Fuzzy sampled-data control for synchronization of T–S fuzzy reaction–diffusion neural networks with additive time-varying delays. *IEEE Trans. Cybern.* **2020**, *51*, 2384–2397. [CrossRef]

31. Thieme, H.R.; Zhao, X.Q. Asymptotic speeds of spread and traveling waves for integral equations and delayed reaction–diffusion models. *J. Differ. Equ.* **2003**, *195*, 430–470. [CrossRef]

32. Yang, X.; Yu, J.; Xu, M.; Fan, W. Convertible bond pricing with partial integro-differential equation model. *Math. Comput. Simul.* **2018**, *152*, 35–50. [CrossRef]

33. Volpert, V.; Petrovskii, S. Reaction–diffusion waves in biology. *Phys. Life Rev.* **2009**, *6*, 267–310. [CrossRef] [PubMed]

34. Halatek, J.; Frey, E. Rethinking pattern formation in reaction–diffusion systems. *Nat. Phys.* **2018**, *14*, 507–514. [CrossRef]

35. Ebenbeck, M.; Knopf, P. Optimal control theory and advanced optimality conditions for a diffuse interface model of tumor growth. *ESAIM Control Optim. Calc. Var.* **2020**, *26*, 71. [CrossRef]

36. Deutscher, J.; Kerschbaum, S. Backstepping control of coupled linear parabolic PIDEs with spatially varying coefficients. *IEEE Trans. Autom. Control* **2018**, *63*, 4218–4233. [CrossRef]

37. Deutscher, J.; Kerschbaum, S. Robust output regulation by state feedback control for coupled linear parabolic PIDEs. *IEEE Trans. Autom. Control* **2019**, *65*, 2207–2214. [CrossRef]

38. Liu, W.W.; Wang, J.M.; Guo, W. A backstepping approach to adaptive error feedback regulator design for one-dimensional linear parabolic PIDEs. *J. Math. Anal. Appl.* **2021**, *503*, 125310. [CrossRef]

39. Seuret, A.; Gouaisbaut, F. Jensen's and Wirtinger's inequalities for time-delay systems. *IFAC Proc.* **2013**, *45*, 343–348. [CrossRef]

40. Yang, C.; Zhang, A.; Zhang, X.; Liu, Z.; Pang, G.; Qiu, J.; Wen, Y.; Shanshui, S.; Cao, J. SPID control for synchronization of complex PIDE networks with time delays. In Proceedings of the IECON 2017-43rd Annual Conference of the IEEE Industrial Electronics Society, Beijing, China, 29 October–1 November 2017; pp. 5997–6001.